High Transmission Gain Inverted-F Antenna on Low-Resistivity Si for Wireless Interconnect

Y. P. Zhang, L. H. Guo, and M. Sun

***Abstract*—Inverted-F antennas of 2-mm axial length are designed and fabricated on a low-resistivity silicon substrate (10 $\Omega \cdot$ cm) using a post back-end-of-line process. For the first time, their performances are measured up to 110 GHz for wireless interconnects. Results show that a sharp resonance can be seen at 61 GHz for the antenna, and a high transmission gain of -46.3 dB at 61 GHz is achieved from the pair of inverted-F antennas at a separation of 10 mm on a standard 10 $\Omega \cdot$ cm silicon wafer of 750-μm thickness.**

***Index Terms*—Integrated antennas, interchip and intrachip radios, wireless chip area networks.**

I. Introduction

CMOS TECHNOLOGY continuously scales down feature size to improve the speed of operation. At the time of writing, the minimum feature size of MOS transistors has reduced to 90 nm and the speed of operation has exceeded 100 GHz. Such rapid scaling has two profound impacts. First, it enables a much higher degree of integration. Second, it implies a much greater challenge of interconnecting because metal wire width and space are greatly reduced and fundamental material limits are approaching. To surpass these fundamental material limits, a wireless interconnect has been proposed. Floyd *et al.* have demonstrated wireless clock distribution at 15 GHz in 0.18-μm CMOS technology [1]. Zhang has evaluated wireless data transmission at 15 GHz and proposed the concept of wireless chip area networks based on ultrawideband (UWB) radio technology [2]. These studies show that wireless interconnects rely on the transmission gains of integrated antennas. To characterize integrated antennas, Kim *et al.* fabricated dipoles of 2-mm axial length on 10 and 20 $\Omega \cdot$ cm silicon substrates and measured their transmission gains from 10 to 18 GHz. They found that the transmission gains of dipoles increase with frequency and are higher on the 20 $\Omega \cdot$ cm silicon substrate than those on the 10 $\Omega \cdot$ cm silicon substrate [3]. To improve integrated antennas, Rashid *et al.* fabricated dipoles of 2-mm axial length on proton-implanted silicon substrates and measured their transmission gains from 6 to 26.5 GHz. They demonstrated that proton implantation greatly increased the resistivity of silicon substrates and the transmission gains. They confirmed that the transmission gains of dipoles increase with frequency and found that the transmission gains could be maximized for a given resistivity by optimizing the silicon substrate thickness [4]. In this paper, we demonstrate high transmission gain integrated inverted-F antennas for wireless interconnect. Inverted-F antennas of 2-mm axial length were fabricated on low-resistivity silicon substrates (10 $\Omega \cdot$ cm) with the post back-end-of-line (BEOL) process. We describe the design and fabrication of the inverted-F antenna in Section II. We analyze and discuss the measured performance of the inverted-F antenna up to 100 GHz in Section III. Finally, we summarize the conclusions in Section IV.

II. Design and Fabrication of Inverted-F Antenna

The linear inverted-F antenna consists of a horizontal element, a short-circuited vertical element, and a signal-driven vertical element. One advantage of the inverted-F antenna is that its input impedance can be arranged to have an appropriate value to match the source impedance without using any additional circuit between the antenna and the source. Another advantage of the inverted-F antenna is its performance with both vertical and horizontal polarizations, because the antenna has both vertical and horizontal elements. The layout and top view photograph of the on-chip inverted-F antenna are illustrated in Fig. 1. The test ground-signal-ground (GSG) pads are squares of 80×80 μm. The width of the line elements is 10 μm. Given the technology, the design parameters are L, H, and S. The effective length $(L + H)$ controls the frequency of resonance, whereas the separation distance S can adjust the antenna impedance to match the source. The pitch of our available on-wafer test probes limits S to 100 μm. Most reported integrated antennas for wireless interconnect have 2-mm axial length. Hence, we chose our parameters L, S, and H as 2 mm, 100 μm, and 100 μm, respectively. Fig. 1 also shows the tested die view including transmit antenna 00 and receive antennas 01, 02, and 03.

One of the challenges for on-chip antennas is the large loss due to low-resistivity silicon substrate. It becomes more serious as the frequency increases to the millimeter-wave range. In order to overcome this problem, a proton-implantation process has been developed [4], [5]. It significantly increases the resistivity of the silicon substrate underneath the antenna radiating element from 10 to 10^5 $\Omega \cdot$ cm. The use of a proton-implanted silicon substrate has deviated from mainstream silicon technology, which undoubtedly reduces the level of system integration

Manuscript received October 28, 2005. This work was supported by the Research Grant Council of Hong Kong under Project HKU 7165/05E. The review of this letter was arranged by Editor S. Kawamura.

Y. P. Zhang and M. Sun are with the Integrated Systems Research Laboratory, School of Electrical and Electronic Engineering, Nanyang Technological University, Singapore 639798 (e-mail: eypzhang@ntu.edu.sg; sunm0001@ntu.edu.sg).

L. H. Guo is with the Semiconductor Process Technology Laboratory, Institute of Microelectronics, Singapore 117685 (e-mail: lihui@ime.a-star.edu.sg).

Digital Object Identifier 10.1109/LED.2006.872351

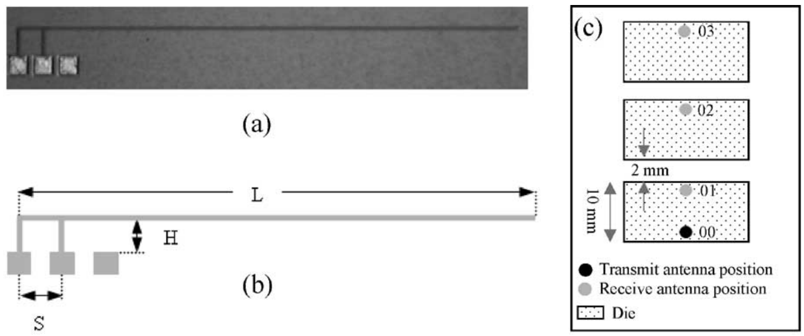

Fig. 1. On-chip inverted-F antenna. (a) Top view photo. (b) Layout. (c) Tested die top view.

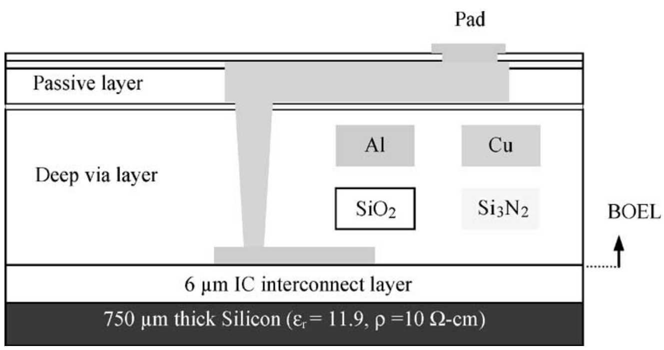

Fig. 2. BEOL process.

and increases the cost of the total solution. In this paper, we employed the post-BEOL process developed at IME for RF CMOS passives to fabricate our antennas. The BEOL process is illustrated in Fig. 2. Note that a standard low-resistivity silicon wafer of 750-μm thickness is used. First, a 6-μm-thick SiO_2 layer is grown on the wafer to simulate the insulator used for on-chip interconnect in standard CMOS process, and over it a 750-nm-thin aluminum pattern is deposited, which is equivalent to the Al pad used in standard CMOS ICs. Then, a 20-μm-thick SiO_2 layer is grown to enhance the isolation of the RF passives from the silicon substrate of low resistivity. The 20-μm-thick SiO_2 layer and the associated deep via capability are two important features of this BEOL process. Next, a 100-nm-thin Si_3N_2 layer is grown. After this process, we proceed to grow a 4-μm-thick SiO_2 layer. In the 4-μm-thick SiO_2 layer, the copper passive pattern is embedded. Deep vias are formed to connect the aluminum with the copper layers. This is followed by sequentially growing a 300-nm-thin Si_3N_2 layer and a 300-nm-thin SiO_2 layer for passivation. The aluminum test pads are finally formed for testing. The inverted-F antenna was fabricated with the simplified post-BEOL process where no aluminum layer was deposited and no deep via was formed. The inverted-F antenna was separated from the silicon substrate by a 20-μm-thick SiO_2 layer.

III. Results and Discussion

The inverted-F antennas were measured on a wafer using a MicroTech probe station and an HP8510XF network analyzer to get the S-parameters in the frequency range of 10–110 GHz.

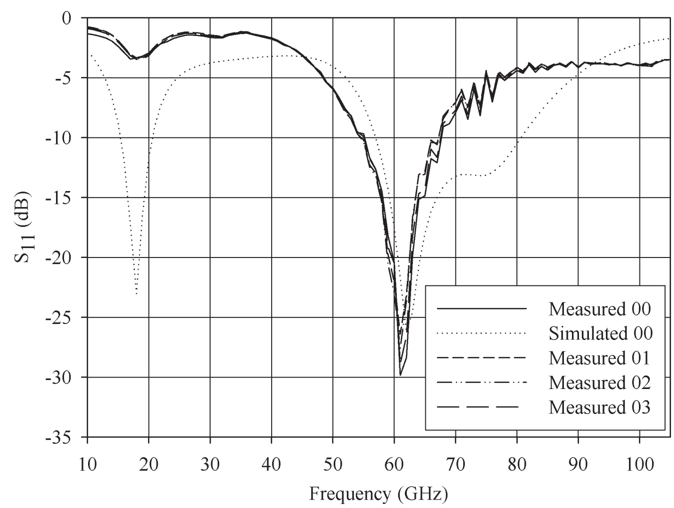

Fig. 3. S_{11} versus frequency.

The wafer was mounted on the metal chuck of the probe station. Transmission gain (TG) is calculated from the S-parameters as [1]

$$\mathrm{TG} = \frac{|S_{21}|^2}{(1-|S_{11}|^2)\,(1-|S_{22}|^2)} \qquad (1)$$

where the symbols have their usual meaning. TG is defined as the antenna transmission gain when the receiving and transmitting antennas are perfectly matched. It is valid only for the case that $S_{11} \ll 1$.

Fig. 3 shows the measured S_{11} results of receive antennas 01, 02, and 03 in Fig. 1 located at three different dies. It is evident that their S_{11} results are insensitive to their location on the wafer. More importantly, it can be seen that a sharp resonance dip occurs at 61 GHz, which indicates the excellent matching of the inverted-F antenna to a 50-Ω source at this frequency. At 61 GHz, the wavelength in a CMOS silicon substrate of low resistivity in Fig. 2 is about 2.2 mm. The feature size of our inverted-F antenna is about 2.2 mm, which indicates that the origin of the 61-GHz resonant frequency comes from the one-wavelength resonance. Using a threshold of -10 dB, a broad 12.5-GHz bandwidth can be achieved at 61 GHz. It is interesting to mention that exploiting the 60-GHz band for wireless local area network applications has recently received considerable attention because at which a large bandwidth of 7 GHz

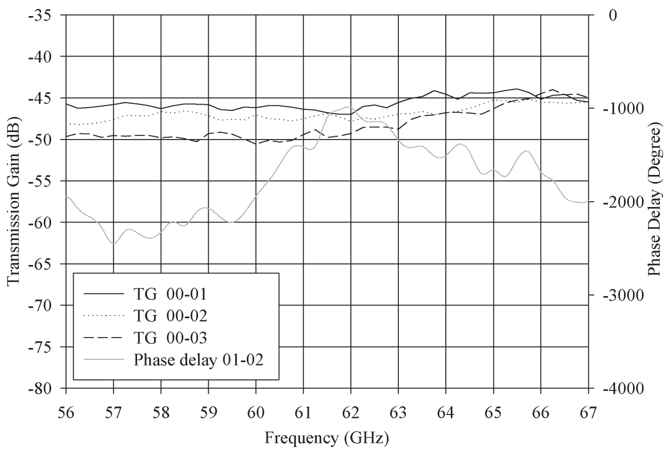

Fig. 4. Transmission gain and phase delay versus frequency.

is available [6]. As the high-frequency capabilities of CMOS technology improve through scaling, CMOS has become a viable technology for 60-GHz operation [7]. In addition, Fig. 3 compares the measured and simulated S_{11} results of the transmit antenna 00 in Fig. 1. The simulation was run using a full-wave solver IE3D. It is seen that the measured and simulated locations of the resonance dips agree well. However, the measured and simulated S_{11} values do not agree well. It might be due to fabrication tolerance.

Fig. 3 shows that the measured S_{11} results are lower than -10 dB in the frequency range of 56–67 GHz, where (1) is valid to use. Fig. 4 shows the calculated transmission gain results in this frequency range between transmit antenna 00 and receive antennas 01, 02, and 03 of Fig. 1. A transmission gain of -46.3 dB at 61 GHz is achieved from the pair of inverted-F antennas at a separation of 10 mm on a standard 10 $\Omega \cdot$ cm silicon substrate of 750-μm thickness. It should be mentioned that a transmission gain of -56 dB was measured for a pair of 2-mm-long and 10-μm-wide dipoles at a separation of 10 mm on a standard 10 $\Omega \cdot$ cm silicon substrate of 500-μm thickness at 18 GHz [1]. This is very close to the -56.3-dB gain at 18 GHz obtained for the same-sized dipoles at the same separation on a standard 10 $\Omega \cdot$ cm silicon substrate of 260-μm thickness [4]. From Fig. 4, it is interesting to note that the transmission gain decreases slowly with the separation distance between the transmit and receive antennas in the far-field region at 61 GHz. An approximate decreasing rate of 0.16 dB/mm reveals that the propagation of guided waves plays a dominant role. Fig. 4 also shows the measured phase delay between receive antennas 01 and 02 with respect to the transmit antenna. It is observed that the phase delay changes rapidly with frequency, which indicates that the signal in this frequency range suffers from the multipath fading due to the propagation of multiple guided modes or paths.

IV. Conclusion

We have designed and fabricated inverted-F antennas of 2-mm axial length on a low-resistivity silicon substrate (10 $\Omega \cdot$ cm) using the BEOL process for wireless interconnects. For the first time, we measured their performance up to 110 GHz. Results show that a sharp resonance can be seen at 61 GHz for the antenna and a high transmission gain of -46.3 dB at 61 GHz is achieved from the pair of inverted-F antennas at a separation of 10 mm on a standard 10 $\Omega \cdot$ cm silicon substrate of 750-μm thickness.

References

[1] B. A. Floyd, C. M. Hung, and K. O. Kenneth, "Intra-chip wireless interconnect for clock distribution implemented with integrated antennas, receivers, and transmitters," *IEEE J. Solid-State Circuits*, vol. 37, no. 5, pp. 534–552, May 2002.

[2] Y. P. Zhang, "Bit-error-rate performance of intra-chip wireless interconnect systems," *IEEE Commun. Lett.*, vol. 8, no. 1, pp. 39–41, Jan. 2004.

[3] K. Kim, H. Yoon, and K. O. Kenneth, "On-chip wireless interconnection with integrated antennas," in *IEDM Tech. Dig.*, 2000, pp. 485–488.

[4] A. B. M. H. Rashid, S. Watanabe, and T. Kikkawa, "High transmission gain integrated antenna on extremely high resistivity Si for ULSI wireless interconnect," *IEEE Electron Device Lett.*, vol. 23, no. 12, pp. 731–733, Dec. 2002.

[5] K. T. Chan, A. Chin, Y. P. Chen, Y. D. Lin, T. S. Duh, and W. J. Lin, "Integrated antennas on Si, proton-implanted Si and Si-on-Quartz," in *IEDM Tech. Dig.*, 2001, pp. 903–906.

[6] *IEEE Standard for Local and Metropolitan Area Networks, Part 16–Air Interface for Fixed Broadband Wireless Access Systems*. (2001). IEEE Standard 802.16. [Online]. Available: http://standards.ieee.org

[7] C. H. Doan, S. Emami, A. M. Niknejad, and R. W. Brodersen, "Design of CMOS for 60 GHz applications," in *Proc. IEEE Solid-State Circuits Conf.*, 2004, pp. 440–449.

射 频 和 天 线 设 计 培 训 课 程 推 荐

易迪拓培训(www.edatop.com)由数名来自于研发第一线的资深工程师发起成立，致力并专注于微波、射频、天线设计研发人才的培养；我们于 2006 年整合合并微波 EDA 网(www.mweda.com)，现已发展成为国内最大的微波射频和天线设计人才培养基地，成功推出多套微波射频以及天线设计经典培训课程和 ADS、HFSS 等专业软件使用培训课程，广受客户好评；并先后与人民邮电出版社、电子工业出版社合作出版了多本专业图书，帮助数万名工程师提升了专业技术能力。客户遍布中兴通讯、研通高频、埃威航电、国人通信等多家国内知名公司，以及台湾工业技术研究院、永业科技、全一电子等多家台湾地区企业。

易迪拓培训课程列表：http://www.edatop.com/peixun/rfe/129.html

射频工程师养成培训课程套装

该套装精选了射频专业基础培训课程、射频仿真设计培训课程和射频电路测量培训课程三个类别共 30 门视频培训课程和 3 本图书教材；旨在引领学员全面学习一个射频工程师需要熟悉、理解和掌握的专业知识和研发设计能力。通过套装的学习，能够让学员完全达到和胜任一个合格的射频工程师的要求…

课程网址：http://www.edatop.com/peixun/rfe/110.html

ADS 学习培训课程套装

该套装是迄今国内最全面、最权威的 ADS 培训教程，共包含 10 门 ADS 学习培训课程。课程是由具有多年 ADS 使用经验的微波射频与通信系统设计领域资深专家讲解，并多结合设计实例，由浅入深、详细而又全面地讲解了 ADS 在微波射频电路设计、通信系统设计和电磁仿真设计方面的内容。能让您在最短的时间内学会使用 ADS，迅速提升个人技术能力，把 ADS 真正应用到实际研发工作中去，成为 ADS 设计专家...

课程网址： http://www.edatop.com/peixun/ads/13.html

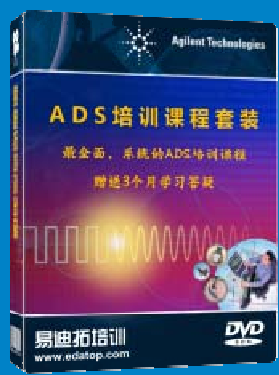

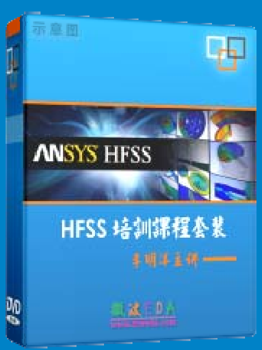

HFSS 学习培训课程套装

该套课程套装包含了本站全部 HFSS 培训课程，是迄今国内最全面、最专业的HFSS培训教程套装，可以帮助您从零开始，全面深入学习HFSS的各项功能和在多个方面的工程应用。购买套装，更可超值赠送 3 个月免费学习答疑，随时解答您学习过程中遇到的棘手问题，让您的 HFSS 学习更加轻松顺畅…

课程网址：http://www.edatop.com/peixun/hfss/11.html

CST 学习培训课程套装

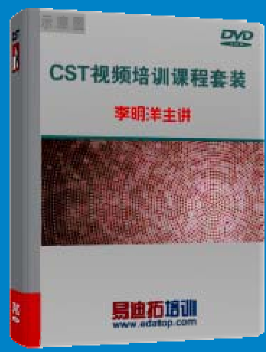

该培训套装由易迪拓培训联合微波 EDA 网共同推出，是最全面、系统、专业的 CST 微波工作室培训课程套装，所有课程都由经验丰富的专家授课，视频教学，可以帮助您从零开始，全面系统地学习 CST 微波工作的各项功能及其在微波射频、天线设计等领域的设计应用。且购买该套装，还可超值赠送 3 个月免费学习答疑…

课程网址：http://www.edatop.com/peixun/cst/24.html

HFSS 天线设计培训课程套装

套装包含 6 门视频课程和 1 本图书，课程从基础讲起，内容由浅入深，理论介绍和实际操作讲解相结合，全面系统的讲解了 HFSS 天线设计的全过程。是国内最全面、最专业的 HFSS 天线设计课程，可以帮助您快速学习掌握如何使用 HFSS 设计天线，让天线设计不再难…

课程网址：http://www.edatop.com/peixun/hfss/122.html

13.56MHz NFC/RFID 线圈天线设计培训课程套装

套装包含 4 门视频培训课程，培训将 13.56MHz 线圈天线设计原理和仿真设计实践相结合，全面系统地讲解了 13.56MHz 线圈天线的工作原理、设计方法、设计考量以及使用 HFSS 和 CST 仿真分析线圈天线的具体操作，同时还介绍了 13.56MHz 线圈天线匹配电路的设计和调试。通过该套课程的学习，可以帮助您快速学习掌握 13.56MHz 线圈天线及其匹配电路的原理、设计和调试…

详情浏览：http://www.edatop.com/peixun/antenna/116.html

我们的课程优势：

※ 成立于 2004 年，10 多年丰富的行业经验，

※ 一直致力并专注于微波射频和天线设计工程师的培养，更了解该行业对人才的要求

※ 经验丰富的一线资深工程师讲授，结合实际工程案例，直观、实用、易学

联系我们：

※ 易迪拓培训官网：http://www.edatop.com

※ 微波 EDA 网：http://www.mweda.com

※ 官方淘宝店：http://shop36920890.taobao.com